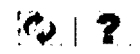


Document Discussion



Return To Library > Records > ERID-92000 through ERID-92999 > ERID-092040 1) HYDROLOGIC BEHAVIOR OF UNSATURATED, FRACTURED TUFF: INTERPRETATION AND MODELING OF A WELLBORE INJECTION TEST

Document Number: 04192006-INNU-P10Z
Created By: Maria E. Romero
Date Created: 04/19/2006 10:16:28 AM
File name: Target-ERID #.pdf
Version: 2.0
Document Type: RPF Record
Document State: Released
Description: REFERENCE CITED; SUBMITTED BY MABLE AMADOR; PUBLISHED IN VADOSE ZONE JOURNAL, VOL. 4, AUGUST 2005

Document Details:

Title: ERID-092040 1) HYDROLOGIC BEHAVIOR OF UNSATURATED, FRACTURED TUFF: INTERPRETATION AND MODELING OF A WELLBORE INJECTION TEST

ERID Number.StartPage: ERID-092040

Office of Record: ENV-ECR

Date Received: 01/12/2006

Official Use Only: N

Page Count: 13

Record Type: Abstract

Document Date: 05/13/2004

To:(Addressees - Organization)
(separate multiple values with semicolons)

From:(Senders - Organization)
(separate multiple values with semicolons) BRUCE A. ROBINSON, STEPHEN G. MCLIN, AND HARI S. VISWANATHAN

Other Document Number(s): N/A
(separate multiple values with semicolons)

TA: N/A
separate multiple values with semicolons)

PRS Number(s): N/A
(separate multiple values with semicolons)

Record Box Number:

Denotes Fields that are mandatory.

To download this file, right mouse click on the file and select 'Save to Disk' or 'Save
[Target-ERID #.pdf](#) <-- This link points to this version.
To check-out and/or edit this file, select Edit Document or Check Out Document from the Document menu above.

31145



Hydrologic Behavior of Unsaturated, Fractured Tuff: Interpretation and Modeling of a Wellbore Injection Test

Bruce A. Robinson,* Stephen G. McLin, and Hari S. Viswanathan

ABSTRACT

A previously reported injection zone test in the Tshirege Member of the Bandelier tuff has been interpreted and modeled using a variety of conceptual models ranging from a single continuum model (SCM) to a dual permeability model (DKM). The agreement of the numerical models and the data was quite acceptable, both qualitatively and quantitatively. The migration of water injected in an open interval of the wellbore exhibited flow that was controlled by gravity and, to a lesser extent, capillary forces. A sensitivity analysis showed that the behavior is well captured with laboratory determined hydrologic parameters and less so if rocks with higher capillary suction are simulated. More complex model formulations that explicitly account for fractures were also tested, but it was found that these models reproduce the field behavior only when parameters are selected that minimize the role of fractures. Therefore, the SCM is favored due to its simpler formulation and ease with which it is implemented in large-scale flow and transport simulations. Discrete fracture simulations are used to illustrate that fractures are predicted to play a minor role in most subunits of the Bandelier tuff: high matrix permeability allows water entering fractures to quickly imbibe into the matrix, thereby reducing the tendency of these rocks to exhibit preferential fracture flow. In contrast, water flow through Basalts present on the Pajarito Plateau is predicted to be dominated by fractures.

RISK INVESTIGATIONS, development of monitoring programs, or strategies for remediation of contaminated groundwater require a quantitative understanding of the relevant groundwater flow and transport processes. This understanding is usually obtained through numerical models of fluid flow and contaminant transport. At Los Alamos National Laboratory (LANL) many released contaminants are present in fluids still residing in the unsaturated zone. Therefore, attaining a predictive capability for flow and transport behavior in the unsaturated zone is critical to the success of models. Characterization of the subsurface hydrology and transport in the unsaturated zone to the degree needed to develop realistic flow and transport models is a challenging activity, given the wide range of recharge rates, the presence of perched water, and the introduction of a host of contaminants of different chemical properties.

As a step toward developing a predictive tool to simulate contaminant migration at LANL, this study examines different conceptual models of unsaturated ground-

water flow for the Bandelier tuff. These tuffs are multiple-flow ash-flow sheets that are typically the first unit exposed on the mesas and most canyons of the Pajarito Plateau. There are various degrees of welding within the tuff units, and many of the subunits contain fractures that must be considered as possible fast pathways. If water percolates through the porous and permeability rock matrix, then the Bandelier tuff may provide a significant barrier to contaminant migration. Percolation rates on the Pajarito Plateau have been estimated to be in the range of several hundred millimeters per year beneath wet canyons such as Los Alamos Canyon (Robinson et al., 2005). Under these high-infiltration conditions, if fractures flow, transport velocities are likely to be much more rapid in the vadose zone than if the water percolates through the rock matrix. For this rock to attenuate the infiltration of contaminated groundwater, it must be demonstrated that water percolates through the porous rock matrix rather than channeling through fractures.

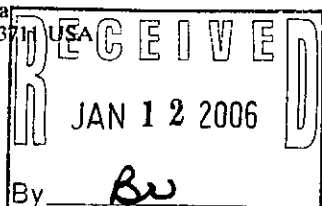
The issue of flow in unsaturated, fractured tuff has been explored both theoretically and experimentally. Nitao and Buscheck (1991) examined an idealized system of parallel, equally spaced fractures with water entering at the top and migrating downward under gravity. They showed that for rocks with large porosities and permeabilities, there is a strong driving force for water to quickly imbibe into the rock matrix. Under these conditions, the water front is quickly attenuated, and in the limit, the downward-migrating wetting front essentially behaves as though the fractures are not present.

Experimentally, Robinson and Bussod (2000) presented unsaturated fluid flow and tracer test results from an experimental facility in tuffs with similar hydrologic properties as the Bandelier tuff. These injection tests indicated that the presence of a fracture in the non-welded, permeable Calico Hills tuff near Yucca Mountain, Nebraska, appeared to have no effect on the migration of water and tracer away from the injection point. Tseng et al. (2003) demonstrated that a SCM formulation could provide a good match to this field data, though scale issues were apparent that could not be readily resolved. In contrast, fast flow through fractures has also been clearly demonstrated in unsaturated, fractured tuffs (e.g., Birdsell et al., 2005). For example, a large-scale fluid and tracer injection experiment in welded, faulted tuff performed by Salve et al. (2004) was dominated by fracture flow. Compared to the Calico Hills tuff, the Salve et al. (2004) test was conducted in welded tuff with orders-of-magnitude lower matrix permeability. This dichotomy of behavior depending on the properties of the fracture and matrix illustrates the importance of laboratory and field investigations to en-

B.A. Robinson and H.S. Viswanathan, Earth and Environmental Sciences Division, Los Alamos National Laboratory, Los Alamos, NM 87545; S.G. McLin, Environmental Stewardship Division, Los Alamos National Laboratory, Los Alamos, NM 87545. Received 13 May 2004. *Corresponding author (robinson@lanl.gov).

Published in Vadose Zone Journal 4:694-707 (2005).
Special Section: Los Alamos National Laboratory
doi:10.2136/vzj2004.0080

© Soil Science Society of America
677 S. Segoe Rd., Madison, WI 53705



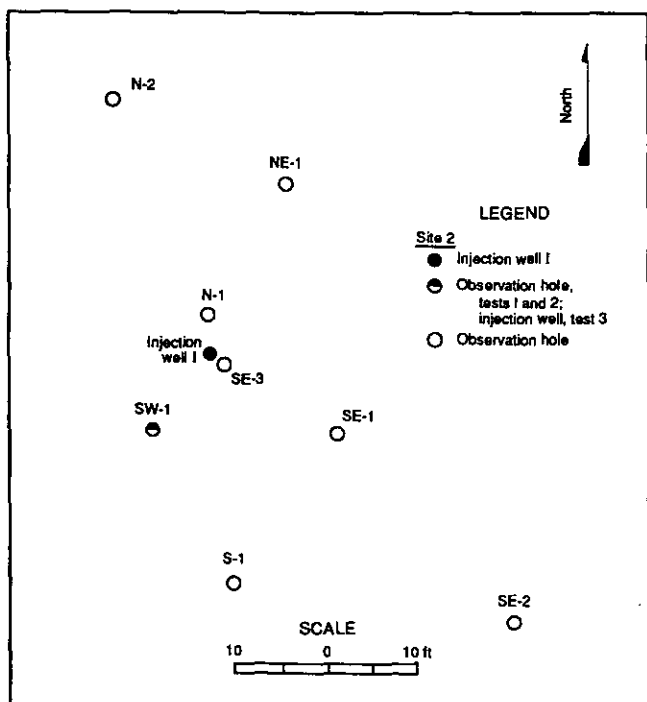


Fig. 1. Locations of injection and monitoring wells for the unsaturated zone injection test. From Purtymun et al. (1989).

sure that the models appropriately account for the role of fractures.

Several conceptual approaches for simulating unsaturated flow and transport in fractured tuff systems have been attempted. With varying degrees of assumption, each method seeks to capture the role of fractures while including the effects of solute diffusion from the fracture into the matrix. Each method has its trade-offs between the realism with which the actual physical system is represented, the available data characterizing the system and processes, and the efficiency and applicability of the numerical method. Ranked from the most physically complex to the most simplified, the methods considered in previous studies include discrete fracture models (DFM, Nitao and Buscheck, 1991; Soll and Birdsell, 1998), DKMs (Bandurraga and Bodvarsson, 1999; Tseng and Zyvoloski, 2000), equivalent continuum models (ECM, Peters and Klavetter, 1988; Pruess et al., 1990), and SCMs.

The present study examines the results of a water injection test performed in the vadose zone at Los Alamos and reported by Purtymun et al. (1989). Through a series of measurements of water migration and accompanying modeling, we demonstrate that the movement of water through the unsaturated zone is a process that can be captured using relatively straightforward numerical models. In the process of performing the modeling, we also explore the relative merits of the different conceptual models listed above for characterizing flow in unsaturated, fractured media. This exercise clarifies the role of fractures in this hydrogeologic setting and provides the basis for the simplifications used in flow and contaminant transport studies performed for the LANL site.

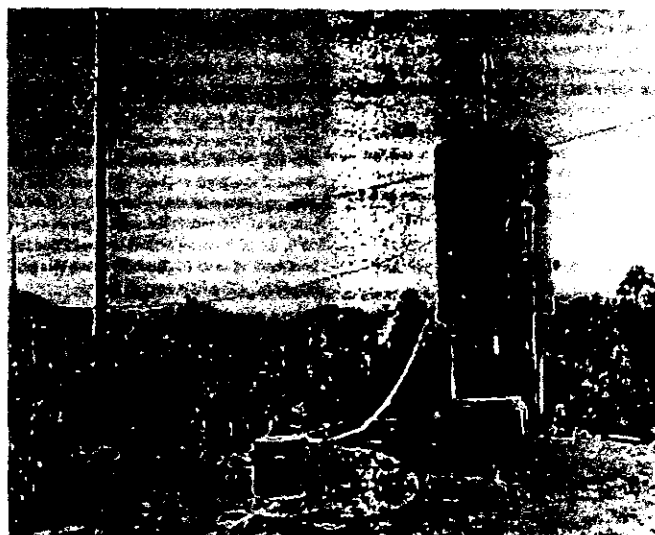


Fig. 2. Injection system used in the unsaturated zone injection test. From Purtymun et al. (1989).

WATER INJECTION TESTS IN THE UNSATURATED BANDELIER TUFF

In the 1960s, LANL and the U.S. Geological Survey conducted a series of water injection tests, using uncontaminated water, to explore the possible use of vadose zone injection wells for water disposal. The method was never used at LANL for water disposal, but data collected from injection tests can be used to understand the hydrologic processes controlling the movement of water in the unsaturated Bandelier tuff. A report by Purtymun et al. (1989) presents water content monitoring data tracking the migration of water from the injection well to the surrounding tuff. These data are modeled in the present study.

Detailed descriptions of the testing methodology, layout, and measurement techniques are presented in Purtymun et al. (1989), so only a brief summary is given here. The complex of injection and observation wells is located on a narrow mesa adjacent to Technical Area 50 (TA-50), the site of LANL's radioactive liquid waste treatment facility. These wells, shown in map view in Fig. 1, are all completed in the upper Tshirege Member, in unit Qbt3. After a few preliminary tests, three longer duration injections were performed in which water content monitoring was performed to track the movement of fluids through the unsaturated tuffs.

The test for which numerical modeling is performed in the present study (referred to as "Test 1 at Site 2" in Purtymun et al., 1989), consists of an injection period of 89 d. The injection system used for the test is shown in Fig. 2. Water from municipal water sources was pumped into a 1892.7-L (500-gallon) storage tank, which discharged into a smaller drum controlled with a float valve to maintain a constant pressure at the ground surface. The 12.7-cm (5-inch) diameter injection well was completed to a depth of 19.8 m (65 feet), with gravel located in the injection zone from 16.8 to 19.8 m (55 to 65 feet), and cement above and below. The 3.18-cm (1.25-inch) injection pipe was fitted with a perforated endpiece to

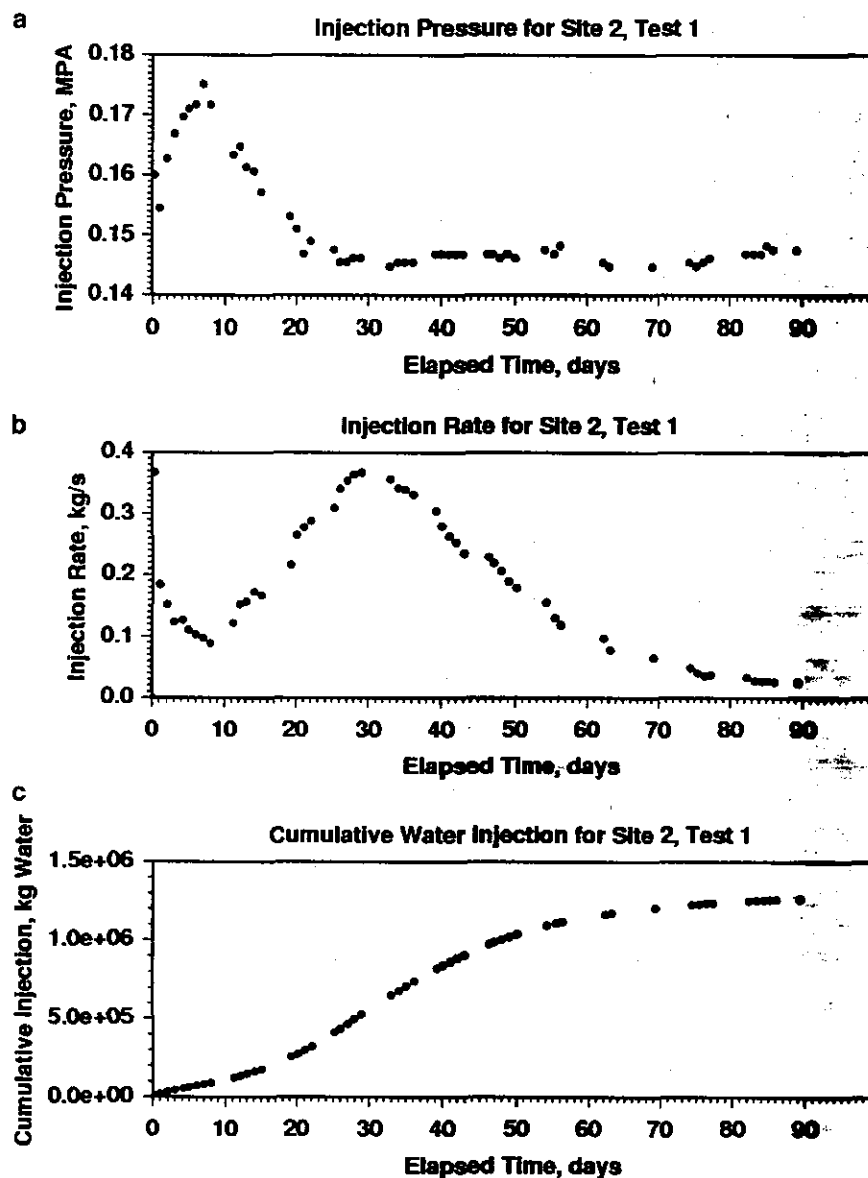


Fig. 3. Measured flow conditions during the unsaturated zone injection test (Site 2, Test 1 of Purtymun et al., 1989). (a) Downhole injection pressure versus time. (b) Injection flow rate versus time. (c) Cumulative mass of water injected during the test.

distribute the flow. A second pipe was also installed to monitor the downhole pressure.

The measured flow conditions during the test are represented in Fig. 3. Despite the constant pressure controlled at the surface, the injection-zone pressure (Fig. 3a) exhibited variations within the first 20 d before stabilizing for the remainder of the injection period. In general, the injection rate (Fig. 3b) was inversely proportional to the pressure. Purtymun et al. (1989) cite possible causes to be variations in atmospheric temperature and pressure, and dissolved gas in the injected fluid. We view these effects to be of relatively minor consequence for the purpose of the study, which is to monitor and model the large-scale migration of fluid through the unsaturated zone. For modeling purposes, the time-dependent injection rate of Fig. 3b is used as direct input. The cumulative mass of water injected versus time is shown Fig. 3c. A total of 1.27×10^6 kg of water

was injected during the 89-d injection phase of the experiment.

Water content monitoring was performed using neutron logs of the surrounding wells (see Fig. 1). These data were used by Purtymun et al. (1989) in two ways. First, data from wells N-1 and SE-3, located close to the injection well, were used directly to determine the rates of movement vertically upward and downward from the injection region. These data are presented with the model comparison in the next section. Also, data from all wells were used to measure the extent of lateral migration and to construct representative cross-sections of water content at various times. These cross-sections were constructed by projecting the results from all boreholes onto a single cross-section. Cross-sections constructed from data at 7, 29, 55, and 89 d after the start of injection, as well as one at Day 327, some eight months after injection was stopped, are shown in Fig. 4

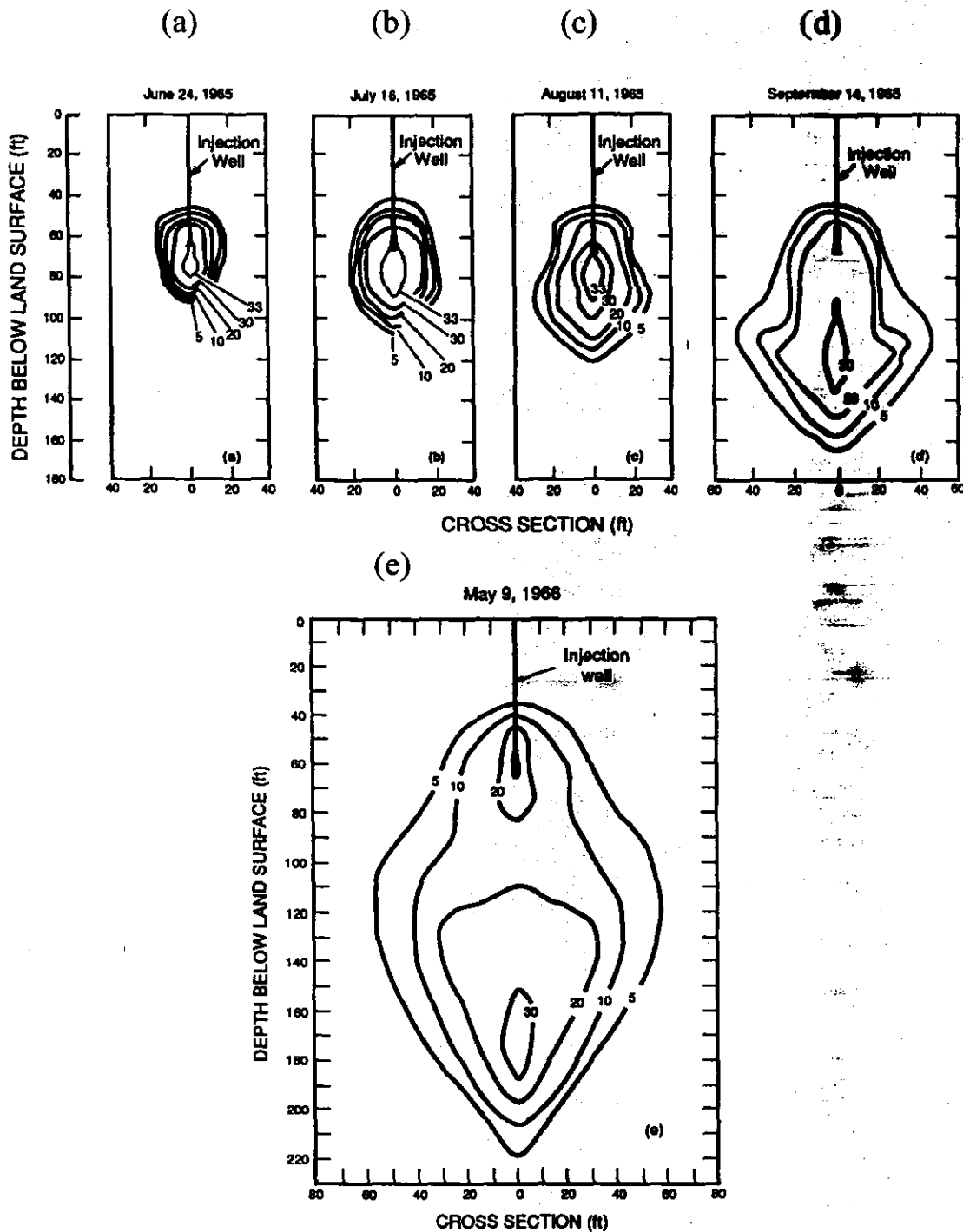


Fig. 4. Contours of water content constructed from the neutron log data during and after the injection test. (a) Day 7 after injection; (b) Day 29; (c) Day 55; (d) Day 89 (end of injection phase); (e) Day 327 (post-injection phase). From Purtymun et al. (1989).

(reproduced from Purtymun et al., 1989). As a check of the validity of these two-dimensional representations of the data, Purtymun et al. (1989) also confirmed that the integrated amount of injected water implied by the constructed cross-section agreed closely with the known amount of water injected. Therefore, all injected water is approximately accounted for in the cross-sections shown.

The use of neutron logging to measure water migration deserves further comment. The goal of the paper

is to determine whether fractures play an important role in the flow of water under unsaturated conditions in this tuff. However, we must recognize that direct measurements of water in the fractures are not possible because the low fracture porosity and water contents are unlikely to be detected, the analysis instead providing an average water content in the matrix and fractures. Therefore, the analysis and modeling hinges on being able to reproduce the large-scale moisture patterns in response to the water injection. We will compare overall

predicted water content distributions in the rock matrix to the measured values, and draw inferences from the models regarding the mechanism of fluid flow.

CONCEPTUAL MODELS FOR FLOW IN UNSATURATED FRACTURED TUFFS

In this section we describe the various conceptual models tested in the present study for interpreting the water injection test.

Single Continuum Model

This model is one in which fractures play no role and only the matrix properties are used for the medium, which could be homogeneous or heterogeneous but without fractures. We refer to this option as the SCM formulation.

Equivalent Continuum Model

The ECM simply attempts to capture characteristics of both the fractures and matrix with a single set of properties. The primary assumption in the model is that the capillary pressure in the fractured medium equals that in the matrix. Assuming the fracture and matrix domains can each be described using a moisture retention and relative permeability model such as that of van Genuchten (1980), the composite permeability of the medium at a given matrix saturation and capillary pressure can be represented as a weighted average of the permeabilities of the two media. For typical properties, the fractures will be predicted to be dry until the capillary pressure in the matrix reaches a low value (at high saturation). This means that the liquid-phase permeability is dominated by matrix properties until almost complete saturation of the matrix, after which fracture saturations and liquid permeabilities rise due to fracture flow. Therefore, in many instances the ECM will behave almost identically to the SCM. Limits of the applicability of the ECM for fluid flow were explored by Pruess et al. (1990). Equivalent continuum model formulations have also been used extensively to simulate two-phase, heat-driven transport of water and air (e.g., Tsang and Pruess, 1987, Buscheck and Nitao, 1993, Buscheck et al., 1996).

Dual Permeability Model

The DKM operates on the assumption that the fractures and matrix material can be represented as two separate, but coupled continua. In the DKM method, both the fracture and matrix domains are discretized using the same numerical grid, giving rise to two individual continua with a one-to-one mapping of grid points between each domain. At each grid point, the matrix is also coupled to the fractures through a first-order interaction term. Hydrologic properties of each continuum are specified, and an additional parameter, the characteristic matrix length scale, is also required. When this length is small, the model reverts to ECM behavior. For larger lengths, the coupling between the fracture and matrix domains becomes weak, and flow in the two

media becomes more independent and uncoupled. The DKM is a suitable model for large-scale simulation because of the practical limitations of models that explicitly represent the fractures as planar features (see below). Therefore, the DKM has been used extensively in studies of dual-porosity soils (e.g., Gerke and van Genuchten, 1993) and for large-scale unsaturated zone flow and transport modeling (Ho, 1997; Viswanathan et al., 1998; Bandurraga and Bodvarsson, 1999; Robinson and Bussod, 2000; Wu and Pruess, 2000).

Discrete Fracture Model

The discrete fracture representation embeds fractures with distinct hydrologic properties within a model domain that includes the rock matrix. A numerical model of such a system requires an extremely high-resolution numerical grid to represent the full structure of the fractures as well as the interaction of the fractures with the rock matrix. Because of the computational burden of the DFM, large-scale modeling efforts such as three-dimensional flow and transport models typically do not utilize the DFM formulation. In this paper, we present a set of idealized simulations that use a DFM to identify the behavior of fracture-matrix interactions in various rock types found beneath the Pajarito Plateau. The simulations provide insight into the flow behavior under unsaturated conditions.

In this study, all of these conceptual models except the DFM are tested using the same numerical grid, boundary conditions, and hydrologic properties, with the goal of matching the characteristics of the water injection test. For the DFM, because there is insufficient basis in field data to warrant the construction of a detailed, single- or multiple-fracture model, we perform idealized calculations to examine the hydrologic behavior for water injected directly into a fracture in the Bandelier tuff under unsaturated conditions to provide a mechanistic explanation for unsaturated flow in these rocks.

NUMERICAL MODEL

Governing Equations for Flow

We use the computer code FEHM (Finite Element Heat and Mass Transfer Code) for the development of the modeling performed in this study. Detailed derivations of the governing equations for two-phase flow as implemented in FEHM have been described previously (e.g., Zyvoloski, 1983; Tseng and Zyvoloski, 2000). FEHM is a two- or three-dimensional finite element code suitable for simulating systems with complex geometries that arise when modeling subsurface flow and transport. In the unsaturated zone, the system of governing equations arises from the principles of conservation of water and air. The conservation of mass for water is expressed by the equation

$$\frac{\partial A_m}{\partial t} + \bar{\nabla} \cdot \bar{f}_m + q_m = 0 \quad [1]$$

where the mass per unit volume, A_m , is given by

Table 1. Hydrogeologic properties used in the models.†

Hydrogeologic unit	Geologic designation	Permeability	Porosity	van Genuchten α parameter	Residual saturation (S_r)	Maximum saturation (S_{1max})	van Genuchten n parameter
		m^2		m^{-1}			
Unit 3	Qbt3	4.79×10^{-13}	0.38	0.594	0.021	0.706	2.16
Unit 2	Qbt2	9.18×10^{-14}	0.33	0.332	0.017	0.821	2.25
Vitric unit	Qbt1v	2.65×10^{-13}	0.38	0.44699	0.005	0.920	1.83
Glassy unit	Qbt1g	3.06×10^{-13}	0.54	0.818	0.000	0.962	1.57
Cerro Toledo	Qct	8.82×10^{-13}	0.47	1.52	0.01	1.	1.506
Cerro del Rio Basalt (DFM model)	Qb4	1.00×10^{-18}	0.05	0.1	0.066	1.	2.
Fractures (for ECM and DKM models)		$1. \times 10^{-12}$	0.001 (fracture volume fraction) 1.000 (within fracture domain)	5.	0.03	1.	1.5

† Data source for Bandelier tuff matrix properties, Springer (2005).

$$A_m = \phi[S_v \rho_v (1 - \eta_v) + S_l \rho_l (1 - \eta_l)] \quad [2]$$

and the mass flux, \bar{f}_m , is

$$\bar{f}_m = (1 - \eta_v) \rho_v \bar{v}_v + (1 - \eta_l) \rho_l \bar{v}_l \quad [3]$$

Here ϕ is the porosity of the matrix, S is saturation, ρ is density, η is the concentration of the noncondensable gas expressed as a fraction of the total mass, and \bar{v} is velocity. The subscripts v and l indicate quantities for the vapor phase and the liquid phase, respectively. Source and sink terms (such as boreholes, injection wells, or groundwater recharge) are represented by the term q_m .

To complete the governing equations it is assumed that Darcy's Law applies:

$$\bar{v}_l = -\frac{kR_l}{\mu_l} (\nabla P_l - \rho_l \bar{g}) \quad [4]$$

A similar expression applies for the vapor phase. Here k is the permeability, R_l is the liquid-phase relative permeability, μ_l is the liquid viscosity, P_l is liquid pressure, and \bar{g} represents the acceleration due to gravity. The phase pressures are related by $P_v = P_l + P_{cap}$, where P_v and P_{cap} are the vapor-phase and capillary pressures, respectively. For simplicity, the equations are shown for an isotropic medium, though this restriction does not exist in the computer code.

In unsaturated media, the relative permeabilities and capillary pressures can be specified using a variety of characteristic curve models. In the present study, we use the van Genuchten (1980) functions, principally because the available data have been reduced using this model. The van Genuchten relative permeability functions are described by the following formulae:

$$R_l = [1 - (1 - \hat{S}^{1/\lambda})^2] \sqrt{\hat{S}} \quad [5]$$

for $\hat{S} < S_{1max}$, where

$$\hat{S} = \frac{S_l - S_{lr}}{S_{1max} - S_{lr}} \quad [6]$$

Finally, for the vapor phase, $R_v = 1 - R_l$. In these equations, the residual liquid and maximum liquid saturations, S_{lr} and S_{1max} , respectively, are experimentally determined parameters, as is the parameter λ , usually expressed in terms of the van Genuchten parameter n as $\lambda = 1 - 1/n$. The capillary pressure is described by the following equation:

$$P_{cap} = \frac{1}{\alpha_g} [\hat{S}^{-1/\lambda} - 1]^{-\lambda} \quad [7]$$

where α_g is the inverse of the air-entry pressure.

Although the focus of this study is fluid flow, some simulations in the present study also solve the transport of a trace component in the fluid phase to illustrate the flow behavior of the injected fluid. For these simulations, the chemical transport module in the FEHM code is used. This model is a traditional continuum-based solution to the advection dispersion equation. Details are presented in Viswanathan et al. (1998).

DISCRETE FRACTURE MODEL

In this section, we present a set of idealized simulations that utilizes a DFM to evaluate the conditions under which fracture and matrix flow is expected. Although we do not simulate the field test results using a DFM, these results provide insight into the relevant hydrologic processes operating during the test. This model captures the pressure gradients in the rock matrix immediately adjacent to the fracture, and thus can be considered to yield the most realistic representation of the transport of fluid between the fracture and matrix. We also present a DFM for flow through a fractured Basalt in which predominantly fracture flow is expected, to explore the contrasting flow characteristics of these two units present beneath the Pajarito Plateau at the LANL site.

The DFM explicitly discretizes the fracture and matrix material as a two-dimensional domain. The node spacing at the fracture-matrix interface is one-half the fracture aperture (0.001 m) and increases with distance into the matrix domain. The domain is 5 m in the horizontal direction and 20 m in the vertical direction, with water and tracer being injected 2 m from the top of the domain. This type of DFM, modeled using the FEHM code, has been shown to compare closely to analytical solutions for transport in fractured material (Dash et al., 1997).

The matrix properties for these and subsequent modeling were obtained from Springer (2005) from measurements on a series of core samples collected from a site geographically close to the TA-50 injection test. The values cited in Table 1 are mean values of the parameters published in that study. Very little information exists on the hydrologic properties of fractures in the Ban-

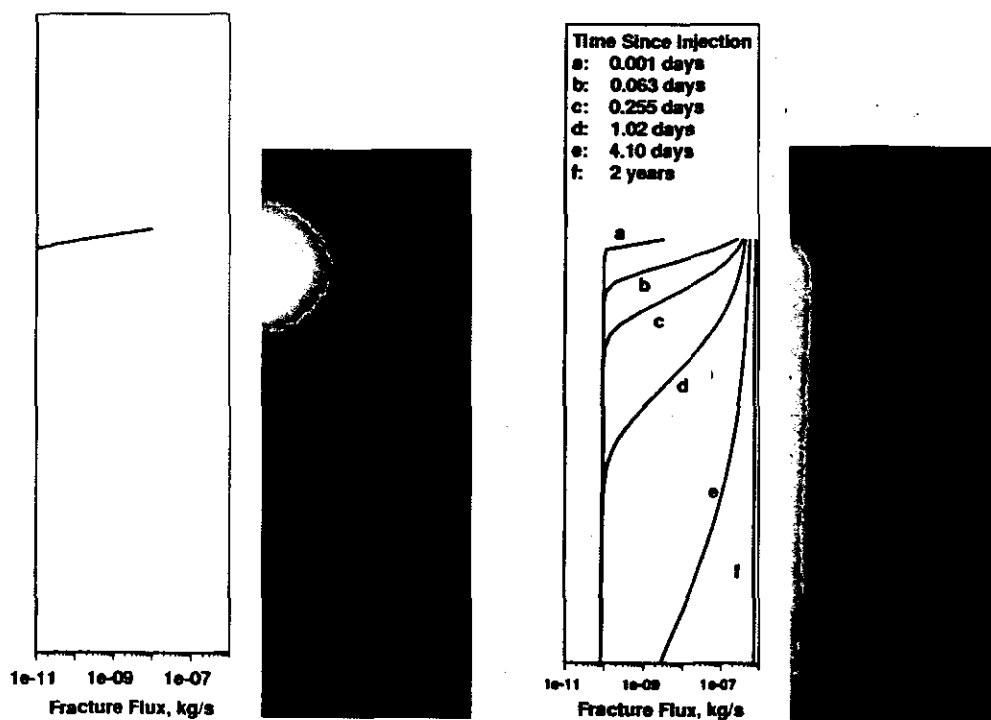


Fig. 5. Discrete fracture model (DFM) simulations. Left: injection into a fracture in the Bandelier tuff, showing the velocities along the length of the fracture and the concentration profile (higher concentrations are represented as white) after two years of injection. Right: DFM for the Basalt, showing preferential flow in the fracture.

delier tuff, principally because the units are fairly sparsely fractured in most locations. In this study we select fracture property values typical of fractured tuffs such as the Yucca Mountain unsaturated zone, to enable us to examine the possible role of fractures at our site. The fracture and matrix properties for the various hydrostratigraphic units present in the model domain are given in Table 1; properties for the Qbt3 unit were selected for these DFM model runs. After a steady state flow field representing background conditions for each hydrostratigraphic unit was achieved, water containing a conservative tracer was injected directly into the fracture of the DFM at rates per unit of depth that are similar to those in the field test. The background conditions were chosen to represent the pre-injection water content values in the tuff before fluid injection.

The simulated concentration profile of the fracture-matrix domain is shown in Fig. 5, alongside a plot of water fluxes within the fracture. Two simulations are shown: a model of the Bandelier tuff (left) and a model of flow through Basalt (right). For the Bandelier tuff case, the fracture flux drops sharply away from the injection point even after two years of injection, indicating that water readily imbibe into the matrix. Consequently, the concentration profile shows that high concentrations are only present in the matrix close to the injection point. If this behavior is present in the field, a single continuum model with matrix properties should be sufficient to describe flow in the Bandelier tuff even when relatively high injection rates are utilized and water is injected directly into a fracture. Matrix-dominated flow occurs readily because of the relatively high matrix permeability, and a capillary suction that is larger than

that of the fracture. This combination results in water imbibition into the matrix.

For comparison, similar plots of the fracture flux profile at various times after injection are shown for the Basalt case in Fig. 5 (right). At very early times, the fracture quickly transmits water vertically downward from the injection point. At times greater than about 4 d, the fracture flux is transmitted all the way down the fracture. This result indicates that fracture flow is likely to play a much more important role in this hydrologic unit. In contrast to the Bandelier tuff, the low matrix permeability of the Basalts makes it impossible for this rock to accept fluid at a rate sufficient to draw injected water into the matrix. Therefore, it flows down the fracture instead.

In summary, the presence of fractures is an insufficient condition for fracture flow to occur under unsaturated conditions. The hydrologic properties of the rock matrix control the ability of water to imbibe into the matrix, under a given water input scenario. This insight is important for understanding the results of the water injection test described in the next section.

NUMERICAL MODELING OF THE FIELD TEST

A three-dimensional numerical grid was constructed to perform the modeling for the test for various conceptual model formulations and parameter sensitivity studies. Top, side, and perspective views of this 53 391 node grid are presented in Fig. 6. Increased horizontal resolution is used to capture the flow system near the injection region. The vertical resolution is also variable to allow

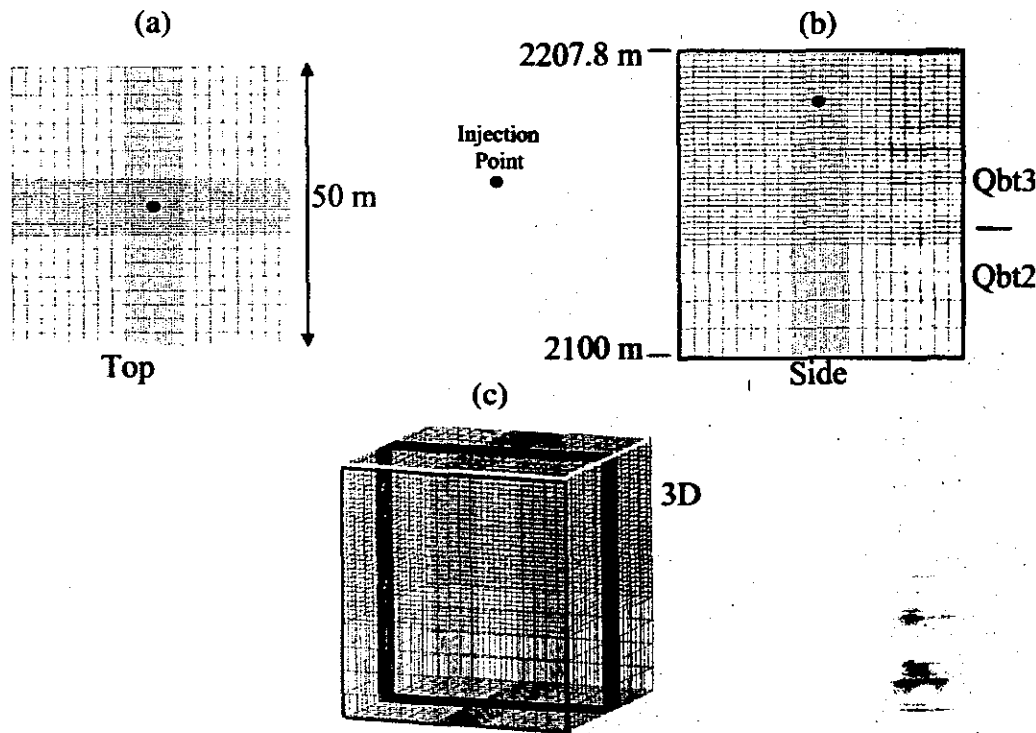


Fig. 6. Numerical grid used in the simulations of the injection test, showing the resolution and the location of the injection interval. (a) Top view. (b) Side view. (c) Perspective view.

the interfaces between the various hydrogeologic layers (shown in Fig. 6b) to be captured. Vertical locations of the layers are based on the geologic model of the LANL site constructed by Carey et al. (1999). At this location on the plateau, the interfaces are close to horizontal, so they are represented this way for simplicity.

The boundary conditions are no-flow on the four vertical faces of the model and constant fluid saturation on the top and bottom. All boundaries are far enough removed from the injection interval that they have no effect on the simulated moisture patterns of the injected fluid. To establish a background flow field suitable for starting the injection simulation, a fluid volumetric water content of 0.05 was set at the top, and the system was run to a steady state condition. This water content is a suitable starting point representative of the pre-injection conditions in the rock mass. Fluid injection is simulated with a source flow rate versus time shown in Fig. 3b, input at a single node at the appropriate location in the model. This approximation is appropriate for simulations focusing on the large-scale migration of the water plume.

Single Continuum Model Results

Two-dimensional cross-sections of volumetric water content through the three-dimensional model at times were prepared (Fig. 7) to allow for a visual comparison to the water plumes constructed from the data (Fig. 4). Many aspects of the measured water migration are captured well by the SCM. Water migrates in all directions, but predominantly downward. Zones of high water content build near the injection point, gravitational

forces pull the plume downward, and capillary forces transmit fluid laterally and, to a limited extent, upward, as the plume grows during the injection (Fig. 7a, 7b, and 7c). There is a noticeable effect, both in the data and the model, of the transition in hydrologic properties at the location of the Qbt3/Qbt2 interface. The formation of two overlapping zones of higher water content, one near the injection point and one within the Qbt2 Formation (Fig. 7c, 7d), is present in both the model and the data. After injection ends, redistribution of water in the rock mass continues during the post-injection monitoring period. The plume continues to migrate downward as well as laterally, resulting in lower water contents spread out over a larger volume (Fig. 7e).

Quantitative comparisons of model and data were made for the SCM conceptualization by comparing the observed and predicted migration rates and distances of the 5% water content front. The model and data comparison is shown in Fig. 8. The red curve and data points represent downward migration rates of the bottom of the injected water plume, where the plotted value represents the average value between the previous data point and the current time. Both model and data show an initial high rate of movement, followed by a tapering off of the rate as the water plume spreads. The black curve is the horizontal movement of the water front at the depth of the injection point, which exhibits a similar trend but starts at slower rates. Since lateral migration is driven principally by capillary forces, the rates are lower than for downward migration to which gravity also contributes. Finally, the blue curve represents the upward location (values on the right axis) to which the

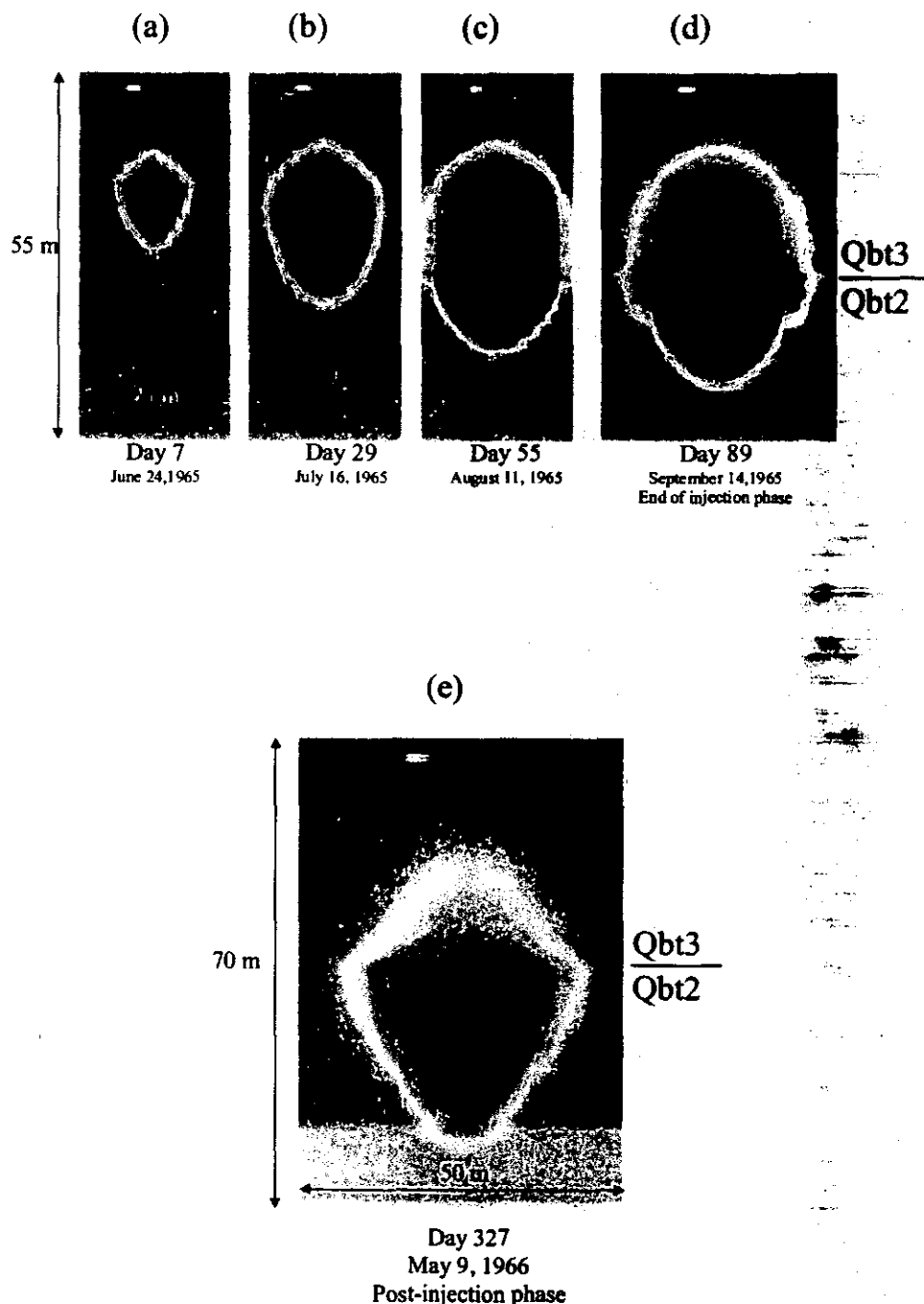


Fig. 7. Two-dimensional cross-sections of water content through the model for various times during the injection test. Times correspond to those at which the cross-sections of Fig. 5 were prepared.

plume migrated at two measurement times, the second being after the eight-month post-injection period. These distances are also controlled by capillary forces, in this case working against gravity. The agreement of model and data for water movement in each direction illustrates that the SCM conceptualization is capable of capturing the key hydrologic processes in effect in the injection test, without explicitly considering fractures.

The preferential downward migration of the water plume is a consequence of the capillary properties of the rock, as controlled principally by the parameter α_g . To demonstrate the sensitivity of the plume behavior

to α_g , model simulations were carried out for the water content profile at Day 55 of the test using the original parameters (Fig. 9a) and α_g values one order of magnitude smaller in all hydrostratigraphic units (Fig. 9b). Clearly, rocks with significantly stronger capillary suction properties (smaller α_g) would yield a more uniform spreading of water in all directions than was observed in the field test. The fact that the laboratory-determined values of α_g reproduced the observed macroscopic plume behavior is evidence that for this system, such measurements can be used to populate a large-scale model of water migration. Scale effects, which in theory

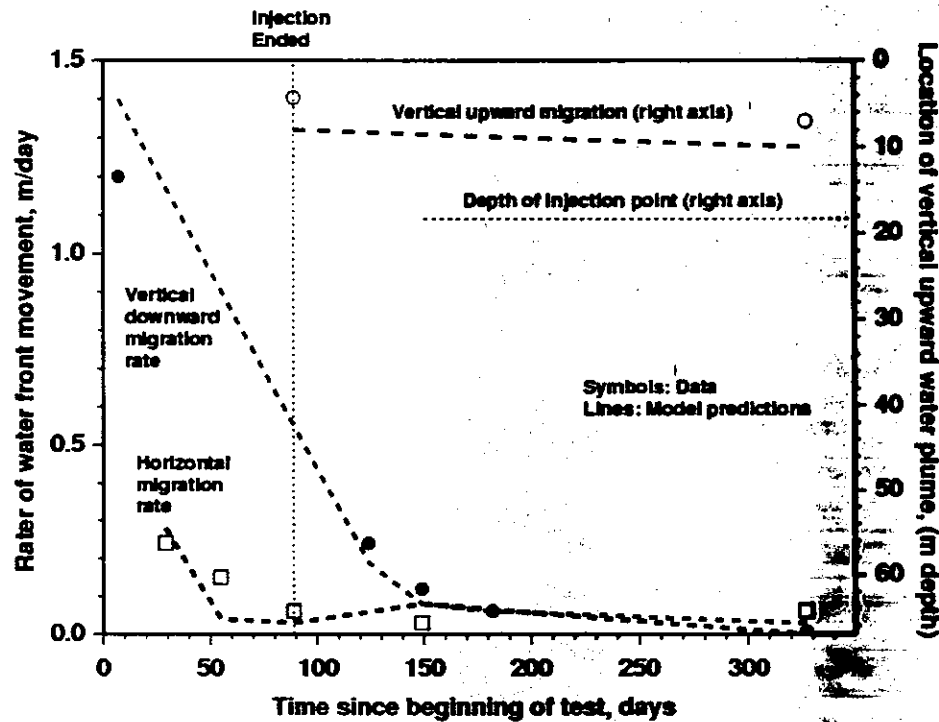


Fig. 8. Predicted and measured rates of water migration vertically downward and horizontally, along with location of upward migration. Symbols, data; lines, model predictions. Curves and points corresponding to the upward migration refer to the right axis.

could have required a revision to the laboratory-determined properties of parameters such as α_e , do not seem to be important for this rock. This result may be specific to the conditions of the test and properties of the rock, and thus may not be transferable to other situations.

Equivalent Continuum Model Results

When fractures are added to the model under the ECM assumption that the capillary pressures in the fractures and matrix are equal, we expect the behavior to be similar to the SCM unless the medium becomes nearly fully saturated. In this experiment, locally saturated conditions are expected near the injection point, raising the potential for fractures to influence the predicted behavior for the ECM formulation. However, a comparison of Fig. 9a and 9c illustrates that the ECM formulation does not significantly impact the predicted large-scale migration of the water plume. There is a very slight tendency for increased downward migration in the ECM prediction, but the effect is small. This model, like the SCM, predicts that the fractures play a very minor role for these hydrologic conditions and rock properties.

Dual Permeability Model Results

Simulations using the DKM formulation were performed assuming that injected fluid enters the system in the fracture continuum. Comparing the ECM and DKM simulations at Day 7 (Fig. 10a, 10b, and 10c), we note that the DKM predicts more rapid downward migration of water as the effective matrix length scale increases. This result is caused by preferential water movement in fractures. The model in Fig. 10b is for a length scale of 0.1 m, a value that yields excellent

communication between the two continua, and an overall water plume migration pattern that matches that of the ECM. The model of Fig. 10c assumes the characteristic matrix length scale is 1-m, which restricts to some extent the ability of water to imbibe into the matrix. This effect was explored further by increasing that length scale to 10 m (Fig. 10d, 10e). The simulated plume within the fracture continuum (Fig. 10e) is predicted to traverse the model domain in one day, a condition not observed in the data. Therefore, for the DKM formulation to resemble the data, unrestricted communication between the fractures and matrix is required, such that water in the fractures imbibes into the matrix. However, for this extreme, a simpler model formulation is the ECM, which is mimicked by the DKM for small values of the matrix length scale parameter.

DISCUSSION AND CONCLUSIONS

An injection zone test in the Tshirege Member of the Bandelier tuff reported by Purtymun et al. (1989) has been interpreted and modeled using different conceptual models that treat the role of fractures in different ways. By putting these different conceptual models to the test against field data, we are able to justify the ultimate selection of numerical model assumptions and parameter values in large-scale numerical simulations. The agreement of data and numerical model assuming the single-continuum model with no fractures was quite acceptable, both qualitatively and quantitatively. The migration of water injected in an open interval of the wellbore exhibited flow that was controlled by both gravity and capillary forces. Flow was preferentially downward, as would be expected under conditions of relatively high flow rate in rocks with low capillary suc-

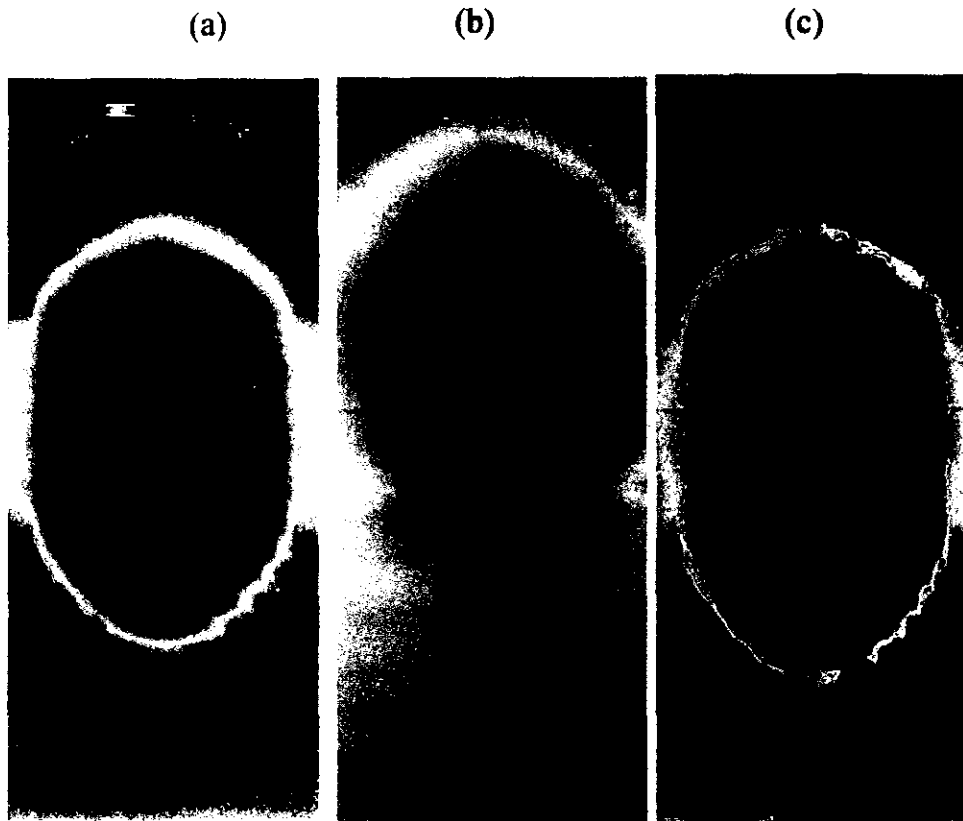


Fig. 9. Two-dimensional cross-sections of water content at Day 55, comparing (a) the single continuum model (SCM), (b) SCM with decreased α_p and (c) equivalent continuum model.

tion. In addition, the effects of an abrupt transition in hydrologic properties at the interface between two tuff subunits were also observed in both the data and the numerical model. The model provided an adequate match to data on the rates of migration of the water plume in the vertical (upward and downward) and lateral directions.

The agreement between the SCM and the data was achieved using hydrologic properties derived from laboratory measurements performed on samples collected from boreholes on the Pajarito Plateau. Recall that the cross-sections constructed by Purtymun et al. (1989) from the water content data could account for all of the injected water. Therefore, it is unlikely that significant flux traveled undetected to greater depths through fractures. These modeling results and the mass balance conclusion of Purtymun et al. (1989) implies that the procedure for populating large-scale numerical models based on hydrologic property measurements made in the laboratory is acceptable. A sensitivity analysis varying the parameter α_p indicates that rocks assumed to possess ten-fold greater capillary suction behavior (a reasonable variability for fractured, welded tuffs) would *not* predict the observed downward plume migration. Therefore, the relatively large α_p values for the Bandelier tuff exert an important influence on the predicted migration of percolating water in these tuffs.

Confirmation that a particular conceptual and numerical model agrees with field-scale data, though encouraging, does not guarantee that other conceptualizations are not also valid. In this study, we also explored models

that explicitly account for **the potential for fractures to influence the flow behavior**. Our model results using the ECM formulation showed water plume migration very similar to the SCM. **The reason for this result is illustrated by our idealized DFM simulations of a discrete fracture with an adjoining porous matrix.** For these rocks, water injected into a fracture preferentially imbibes into the matrix when reasonable fracture hydrologic properties are assumed, and the contact area between fracture water and the matrix is assumed to be unrestricted. Only when the rate of water percolation is too high for the matrix to accept (as in the Basalt case presented for comparison) will the fractures transmit fluid significant distances. The ECM formulation, with its enforced condition of equal pressures in the fracture and matrix, does **not** allow fractures to flow unless the matrix is nearly fully saturated. For this field test, this condition is predicted to occur only very close to the injection point. Therefore, including fractures in an ECM model changes the results only very slightly. Interestingly, it does not appear to be necessary to include these fractures to obtain an adequate match to the large-scale features of the experiment.

The final conceptual model tested was the DKM formulation, which allows a condition of unequal pressures in the two media (fractures and matrix). Not surprisingly, when the parameter controlling the degree of fluid communication between the fracture and matrix was set so as to result in equal pressures in the two media, results similar to the SCM and ECM formulations were obtained. However, when the fractures are assumed to

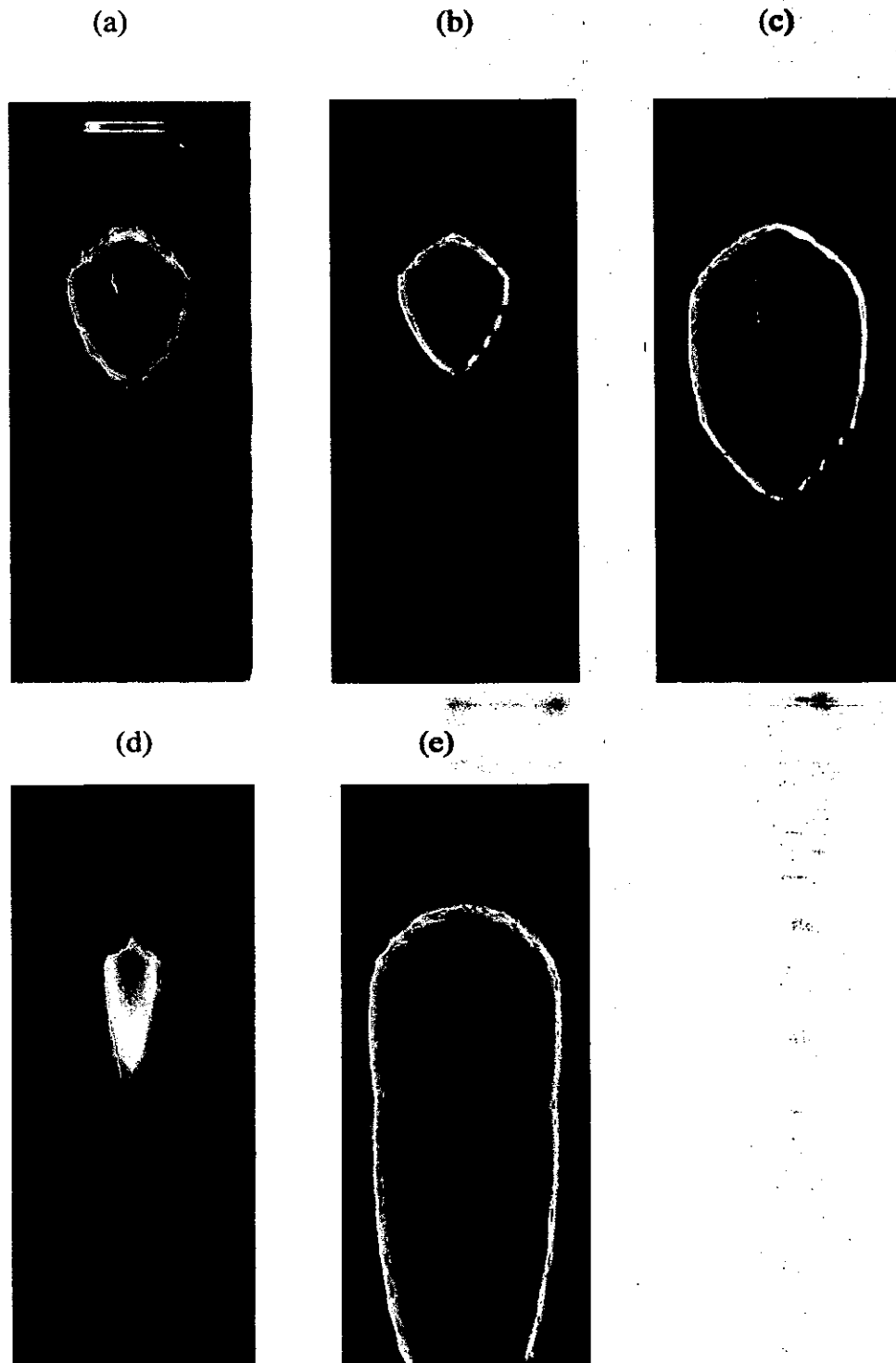


Fig. 10. Two-dimensional cross-sections of water content comparing the equivalent continuum model (ECM) and dual permeability model (DKM) formulations. (a) ECM, Day 7; (b) DKM, Day 7, effective matrix length scale of 0.1 m; (c) DKM, Day 7, effective matrix length scale of 1 m; (d) DKM, after one day of injection, effective matrix length scale of 10 m; (e) fracture water content corresponding to d (color scale is from 0 to 0.1 for this figure only).

be more hydrologically isolated from the matrix, this model predicts an extremely rapid downward percolation of water within a few days, a condition not observed in the data. Therefore, if a DKM formulation were to be selected to model percolation in the Bandelier tuff, good connection between the fracture and matrix should

be assumed. However, there seems to be no motivation to employ a DKM model for these tuffs, since the only way to achieve agreement with the field observations is by making it mimic the SCM or ECM models. Therefore, selecting one of these simpler models is preferable.

The representativeness of the field experimental re-

sults also requires discussion, given that the test is a point-source injection from a wellbore, rather than natural infiltration. We can compute an average downward percolation rate during the test by dividing the fluid injection rate by the cross-sectional area of the water plume at a particular time. Applying this method at Day 55 of injection, we obtain an estimated flux of about 2.7×10^4 mm yr⁻¹. This rate is much higher than estimated infiltration rates of the order of 1000 mm yr⁻¹ for the Pajarito Plateau, even in wet canyons. The implication of this result is that if matrix-dominated flow is observed even at the high percolation rates of this injection test, then it is very likely to be the case under natural infiltration conditions on the Plateau.

With respect to contaminant migration contaminants in fluids percolating through the Bandelier tuff, the consequence of matrix-dominated flow is to decrease travel velocities beyond what would be the case if preferential channeling through fractures were to occur. In addition, matrix-dominated flow increases the likelihood of retardation due to sorption by ensuring good contact between the contaminant and the rock. Qualitatively, the existing information on groundwater contaminant migration from laboratory facilities agrees with this result. There is evidence that some nonsorbing contaminants such as tritium and perchlorate have traveled significant depths through the unsaturated zone, even to the regional aquifer (Rogers, 1998; LANL, 2004) during the 50+ years of laboratory operation. This is probably a consequence of releases into canyons, and transport at high percolation rates through regions where the Bandelier tuff is thin or not present. However, most known contaminant releases have not traveled that far, and thus still reside in the unsaturated zone.

The injection test results and accompanying modeling suggests that unsaturated flow and transport through the Bandelier tuff units tested should be represented using a formulation that favors matrix flow and transport, rather than fracture-controlled transport. This behavior is a consequence of the high matrix permeability of the Bandelier tuff. The relatively low capillary suction properties of the tuff, compared to otherwise similar tuffs present at Yucca Mountain, for example, results in preferential downward percolation through the rock matrix at high percolation rates. In contrast, rocks with higher capillary suction properties would be expected to result in more lateral and spreading of the water plume, whereas low matrix-permeability rocks are expected to result in preferential fracture flow. Therefore, in applying these results to other rock types and hydrologic settings, the matrix hydrologic properties should be compared to those of the Bandelier tuff to assess whether similar mechanisms will exist.

ACKNOWLEDGMENTS

This work was conducted under the auspices of the U.S. Department of Energy, Los Alamos Environmental Restoration Project and the LANL Groundwater Protection Program. The authors also wish to thank the many staff of the laboratory's Environmental Restoration Project for many useful discussions during the course of this work. Special thanks go to

Diana Hollis for supporting the modeling effort and suggesting that this test be used to test the conceptual model presented in this study, and to Kay Birdsell and two anonymous reviewers for their thorough reviews of the work.

REFERENCES

- Bandurraga, T.M., and G.S. Bodvarsson. 1999. Calibrating hydrogeologic parameters for the 3-d site-scale unsaturated zone model of Yucca Mountain, Nevada. *J. Contam. Hydrol.* 38:25-46.
- Birdsell, K.H., B.D. Newman, D.E. Broxton, and B.A. Robinson, 2005, this issue. Conceptual models of vadose-zone flow and transport beneath the Pajarito Plateau, Los Alamos, New Mexico. Available at www.vadosezonejournal.org. *Vadose Zone J.* 4:620-636 (this issue).
- Buscheck, T.A., and J.J. Nitao. 1993. Repository-heat-driven hydrothermal flow at Yucca Mountain: Part I. Modeling and analysis. *Nucl. Technol.* 104:418-448.
- Buscheck, T.A., J.J. Nitao, and L.D. Ramspott. 1996. Localized dryout: An approach for managing the thermal-hydrological effects of decay heat at Yucca Mountain. *Materials Res. Soc. Symp. Proc.* 412:715-722. Materials Research Society, Pittsburgh, PA.
- Carey, B., G. Cole, C. Lewis, F. Tsai, R. Warren, and G. WoldeGabriel. 1999. Revised site-wide geologic model for Los Alamos National Laboratory (FY99). LA-UR-00-2056. Los Alamos Natl. Lab., Los Alamos, NM.
- Dash, Z.V., B.A. Robinson, and G.A. Zylowski. 1997. Software requirements, design, and verification and validation for the FEHM application: A finite-element heat-and-mass transfer code. LA-13305-MS. Los Alamos Natl. Lab., Los Alamos, NM.
- Gerke, H.H., and M.T. van Genuchten. 1993. Evaluation of a first-order water transfer term for variably saturated dual-porosity flow models. *Water Resour. Res.* 29:1225-1238.
- Ho, C.K. 1997. Models of fracture-matrix interactions during multiphase heat and mass flow in unsaturated fractured porous media. p. 401-412. In *Proceedings of the 1997 ASME International Mechanical Engineering Congress and Exposition*, Dallas, TX. 16-21 Nov. 1997. ASME, Fluids Engineering Division.
- LANL. 2004. Environmental surveillance at Los Alamos during 2002. LA-14085-ENV. Los Alamos Natl. Lab., Los Alamos, NM.
- Nitao, J.J., and T.A. Buscheck. 1991. Infiltration of a liquid front in an unsaturated, fractured porous medium. *Water Resour. Res.* 27: 2099-2112.
- Peters, R.R., and E.A. Klavetter. 1988. A continuum model for water movement in an unsaturated fractured rock mass. *Water Resour. Res.* 24:416-430.
- Pruess, K., J.S. Wang, and Y.W. Tsang. 1990. On thermohydrologic conditions near high-level waste emplaced in partially saturated fractured tuff. 1. Simulation studies with explicit consideration of fracture effects. *Water Resour. Res.* 26:1235-1248.
- Purtymun, W.D., E.A. Enyart, and S.G. McLin. 1989. Hydrologic characteristics of the Bandelier tuff as determined through an injection well system. Report LA-11511-MS. Los Alamos Natl. Lab., Los Alamos, NM.
- Robinson, B.A., and G.Y. Bussod. 2000. Radionuclide transport in the unsaturated zone at Yucca Mountain: Numerical model and field validation studies. p. 323-336. In *Geophysical Monograph 122*. Witherspoon Volume. AGU, Washington, DC.
- Robinson, B.A., G. Cole, J.W. Carey, M. Witkowski, C.W. Gable, Z. Lu, and R. Gray. 2005. A vadose zone flow and transport model for Los Alamos canyon, New Mexico. Available at www.vadosezonejournal.org. *Vadose Zone J.* 4:729-743 (this issue).
- Rogers, D.B. 1998. Impact of tritium disposal on surface water and groundwater at Los Alamos National Laboratory through 1997. Report LA-13465-SR. Los Alamos Natl. Lab., Los Alamos, NM.
- Salve, R., H.H. Liu, P. Cook, A. Czamomski, Q. Hu, and D. Hudson. 2004. Unsaturated flow and transport through a fault embedded in fractured welded tuff [Online]. *Water Resour. Res.* 40(4):W04210. doi:10.1029/2003WR002571.
- Soll, W.E., and K.H. Birdsell. 1998. The influence of coatings and fills on flow in fractured, unsaturated porous media systems. *Water Resour. Res.* 34:193-202.
- Springer, E.P. 2005. Statistical exploration of matrix hydrologic properties for the Bandelier tuff, Los Alamos, New Mexico. Available

- at www.vadosezonejournal.org. *Vadose Zone J.* 4:505-521 (this issue).
- Tsang, Y.W., and K. Pruess. 1987. A study of thermally induced convection near a high-level nuclear waste repository in partially saturated fractured tuff. *Water Resour. Res.* 23:1958-1966.
- Tseng, P.-H., W.E. Soll, C.W. Gable, H.J. Turin, and G.Y. Bussod. 2003. Modeling unsaturated flow and transport processes at the Busted Butte field test site, Nevada. *J. Contam. Hydrol.* 62-63: 303-318.
- Tseng, P.H., and G.A. Zyvoloski. 2000. A reduced degree of freedom method for simulating non-isothermal multi-phase flow in a porous medium. *Adv. Water Resour.* 23:731-745.
- van Genuchten, M.Th. 1980. A closed-form solution for predicting the hydraulic conductivity of unsaturated soils. *Soil Sci. Soc. Am. J.* 44:892-898.
- Viswanathan, H.S., B.A. Robinson, A.J. Valocchi, and I. Triay. 1998. A reactive transport model of neptunium migration from the potential repository at Yucca Mountain. *J. Hydrol. (Amsterdam)* 209: 251-280.
- Wu, Y.S., and K. Pruess. 2000. Numerical simulation of non-isothermal multi-phase tracer transport in heterogeneous fractured porous media. *Adv. Water Resour.* 23:699-723.
- Zyvoloski, G. 1983. Finite-element methods for geothermal reservoir simulation. *Int. J. Numer. Anal. Meth. Geomech.* 7:75-86.